



HAL
open science

Impacts of urban stressors on freshwater biofilms

Romain Vrba, Isabelle Lavoie, Nicolas Creusot, Mélissa Eon, Débora Millan-Navarro, Agnès Feurtet-Mazel, Nicolas Mazzella, Aurélie Moreira, Dolores Planas, Soizic Morin

► **To cite this version:**

Romain Vrba, Isabelle Lavoie, Nicolas Creusot, Mélissa Eon, Débora Millan-Navarro, et al.. Impacts of urban stressors on freshwater biofilms. 2023. hal-04173352

HAL Id: hal-04173352

<https://hal.inrae.fr/hal-04173352>

Preprint submitted on 31 Jul 2023

HAL is a multi-disciplinary open access archive for the deposit and dissemination of scientific research documents, whether they are published or not. The documents may come from teaching and research institutions in France or abroad, or from public or private research centers.

L'archive ouverte pluridisciplinaire **HAL**, est destinée au dépôt et à la diffusion de documents scientifiques de niveau recherche, publiés ou non, émanant des établissements d'enseignement et de recherche français ou étrangers, des laboratoires publics ou privés.



Distributed under a Creative Commons Attribution - NonCommercial - NoDerivatives | 4.0 International License

1 Impacts of urban stressors on freshwater biofilms

2 Romain VRBA^{1,2,*}, Isabelle LAVOIE², Nicolas CREUSOT¹, Mélissa EON¹, Débora MILLAN-NAVARRO¹,
3 Agnès FEURTET-MAZEL³, Nicolas MAZZELLA¹, Aurélie MOREIRA¹, Dolors PLANAS⁴, Soizic MORIN¹

5 ¹ INRAE, UR EABX, 50 avenue de Verdun, 33612 Cestas cedex, France

6 ² INRS-ETE, 490 rue de la Couronne, Québec, QC G1K 9A9, Canada

7 ³ Univ. Bordeaux, UMR CNRS 5805 EPOC-OASU, F-336120 Arcachon, France

8 ⁴ UQAM, GRIL-Département des sciences biologiques, 141 Avenue du Président-Kennedy, Montréal,
9 QC H2X 1Y4, Canada

10 *Corresponding author at: INRAE, UR EABX, 50 avenue de Verdun, 33612 Cestas cedex, France.

11 Tel. : +33 6 95 43 84 28

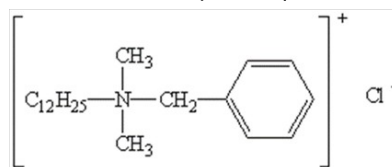
12 E-mail address: romvrba@outlook.fr

13

14 Graphical abstract

15

Dodecylbenzyltrimethylammonium chloride (BAC 12)

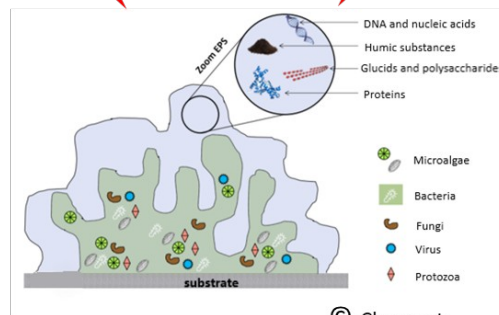


Artificial Light at Night (ALAN)



- *Damage on the phospholipid membrane*
- *Modification of taxonomic composition*

- *Disruption of photosynthetic cycles*



© Chaumet

16

17

18

19

20

21

22 Abstract

23 In urban areas, aquatic ecosystems and their communities are exposed to numerous
24 stressors of various natures (chemical and physical), which impacts are often poorly
25 documented. In epidemic context such as the COVID 19 pandemic, the use of biocides such
26 as the dodecylbenzyltrimethylammonium chloride (BAC 12) increased, resulting in an
27 expectable increase in their concentrations in urban aquatic ecosystems. This compound is
28 known to be toxic to most aquatic organisms. Besides, artificial light at night (ALAN) is
29 increasing globally, especially in urban areas. ALAN may have a negative impact on
30 photosynthetic cycles of periphytic biofilms, which in turn may result in changes in their
31 metabolic functioning. Moreover, studies suggest that exposure to artificial light could
32 increase the biocidal effect of BAC 12 on biofilms. The present study investigates the
33 individual and combined effects of BAC 12 and/or ALAN on the functioning and structure of
34 photosynthetic biofilms. We exposed biofilms to a nominal concentration of 30 mg.L⁻¹ of
35 BAC 12 and/or ALAN for 10 days. BAC 12 had a negative impact on biofilm functioning by
36 decreasing the amount and the quality of photosynthetic pigments, resulting in a >90%
37 decrease in photosynthetic efficiency after 2 days of exposure. We also noted a strong
38 decrease in glycolipids that resulted in a shift in lipid profiles. We found no significant effect
39 of ALAN on the endpoints assessed and no interaction between the two stress factors.

40 **Keywords:** Biocide, ALAN, biofilm, photosynthetic efficiency, bioaccumulation, lipids.

41 **1- Introduction**

42 Today, biocides are widely used in different areas of activity including agriculture and
43 industry, as well as in a multitude of products (e.g. pharmaceutical, personal care and
44 household products) (Abbott et al., 2020). Among these biocides,
45 dodecylbenzyltrimethylammonium chloride (BAC 12), a quaternary ammonium compound, is
46 commonly used as an active substance in medical disinfection products, as well as in
47 household products such as detergents. Recently, following the regulation of some broadly
48 used disinfectant agents such as triclosan, quaternary ammonium compounds like BAC 12
49 have become popular substitutes (Sreevidya et al., 2018). Moreover, BAC 12 and all other
50 benzalkonium chloride derivatives have been shown to be very effective against the SARS-
51 CoV virus (Rabenau et al., 2005), resulting in their widespread use as disinfectants during
52 pandemic. For example, benzalkonium chloride-based disinfectants represented more than
53 half of the products recommended by the US Environmental Protection Agency (EPA) against
54 SARS-CoV-2 (US EPA, 2020).

55

56 Like other contaminants, BAC 12 eventually reaches wastewaters, where its concentration
57 varies greatly depending on the land use, population and wastewater treatment facilities,
58 among other factors. For example, a concentration of 6 mg.L⁻¹ was recorded in hospital
59 effluents (Kümmerer et al., 1997) due to the intensive use of BAC 12 as a disinfectant. In
60 municipal wastewater effluents, BAC 12 concentrations were observed to range from just a
61 few ng.L⁻¹ up to 170 µg.L⁻¹ (Clara et al., 2007; Martínez-Carballo et al., 2007; Zhang et al.,
62 2015). BAC 12 concentration was likely much higher during the Covid-19 pandemic as a
63 result of increased efforts to sanitize all kinds of surfaces. According to the US EPA, BAC 12 is

64 relatively stable to photodegradation and its half-life in surface waters can reach 180 days,
65 although the presence of photosensitizers can reduce this half-life to a week (US EPA, 2006).
66 The K_{oc} of BAC 12 is 5.43 and, therefore, it has a high adsorption ratio on sewage sludge,
67 sediments or humic substances (van Wijk et al., 2009). However, some bacterial strains in
68 wastewaters, such as *Aeromonas hydrophila*, can biodegrade the BAC 12 molecule and use
69 the ammonium as a source of nitrogen (Patrauchan and Oriel, 2003).

70 The toxicity of BAC 12 to cells is due to its quaternary ammonium polar head, which has the
71 capacity to bind to the surface membrane, while the alkyl lipophilic chain alters the
72 phospholipid bilayer. This alteration can rapidly lead to membrane disruption and
73 progressive lysis of the cell (Eich et al., 2000). BAC 12 has attracted attention in medical
74 research because of its widespread use, as some bacterial strains such as *Staphylococcus*
75 *aureus* (Wassenaar et al., 2015) have shown resistance mechanisms. Resistant strains of
76 *Pseudomonas aeruginosa* show some differences in their fatty acid profiles that induce shifts
77 in cell membrane composition (Sakagami et al., 1989; Kim et al., 2018).

78 Although the transfer of BAC 12 to aquatic ecosystems has been recognized, the ecotoxicity
79 of BAC 12 to aquatic organisms is poorly documented. There is redundancy in the organisms
80 used for toxicity assessment, since most studies have focused on *Daphnia magna* to
81 determine the toxicity of BAC 12 (Kreuzinger et al., 2007; Leal et al., 1994; Chen et al., 2014;
82 Lavorgna et al., 2016). To date, *D. magna* is the most sensitive organism to BAC 12, where
83 the concentration needed to immobilize 50% of organisms (EC_{50}) has been shown to be 5.9
84 $\mu\text{g}\cdot\text{L}^{-1}$ (US EPA, 2006). As a result, the US EPA established a non-observed adverse effect
85 concentration (NOAEC) of 4.15 $\mu\text{g}\cdot\text{L}^{-1}$ for aquatic invertebrates. Phytoplanktonic organisms
86 seem to be less sensitive to BAC 12 than aquatic invertebrates. Indeed, several other studies
87 investigated the effects of BAC 12 on various microalgae species and the range of EC_{50} based
88 on growth was found to vary between 58 $\mu\text{g}\cdot\text{L}^{-1}$ for *Skeletonema costatum* (Kreuzinger et al.,
89 2007) to 203 $\mu\text{g}\cdot\text{L}^{-1}$ for *Chlorella vulgaris* (Sütterlin et al., 2008).

90 In this study, we focused on stream biofilms (periphyton), which are complex structures
91 housing autotrophic microorganisms (e.g. cyanobacteria, green algae, diatoms), bacteria,
92 fungi, and other heterotrophic organisms. Biofilms are ubiquitous in aquatic environments,
93 including urban streams and ponds. They can also be found downstream of wastewater
94 treatment plants (WWTPs) and have been used to detect structural and functional changes
95 as a response of microbial communities to stress (Tamminen et al., 2022; Tlili et al., 2020).
96 Diatoms are often the major algal components in biofilms in terms of biomass (Morin et al.,
97 2016). Diatoms are rich in essential polyunsaturated fatty acids such as eicosapentaenoic
98 acid (EPA) (Zulu et al., 2018), ensuring a high nutritional quality of this primary resource for
99 biofilm consumers. Changes in the biofilm community structure could lead to a decrease in
100 essential polyunsaturated fatty acids (Brett and Müller-Navarra, 1993). Recent studies also
101 demonstrated that diatom fatty acid composition can be altered by organic substances such
102 as pesticides (Demailly et al., 2019). Given the toxic mode of action of BAC 12, impacts on
103 biofilm fatty acids, particularly membrane phospholipids, are likely to occur. The attack on
104 phospholipid membrane may also result in the disruption of key functions of biofilm such as
105 photosynthesis for example, Pozo-Antonio and Sanmartin (2018) showed a significant
106 decrease in chlorophyll *a* and photosynthetic efficiency of phototrophic biofilms from church

107 walls after a BAC 12 treatment. The effect of BAC 12 as a biofouling removal agent was
108 significantly enhanced when combined with artificial light or UV irradiation.

109 With urban development, artificial light at night (ALAN) has become a global pollution
110 concern and more than 80% of the world population lives under a light-polluted sky (Falchi
111 et al., 2016). Furthermore, most urban areas have developed along rivers and coastlines,
112 increasing the exposure of aquatic environments to ALAN. Concerns about the impact of
113 ALAN on aquatic ecosystems and research on this topic are quite recent (Perkin et al., 2011).
114 Indeed, ALAN was only recognized as harmful for freshwater ecosystems in the early 2000s
115 (Longcore and Rich, 2004). ALAN could lead to disruptions in photosynthesis-respiration
116 cycles of autotrophic organisms in biofilms by inducing variability in the maximum efficiency
117 of photosynthesis (Maggi and Serôdio, 2020). ALAN can also alter taxonomic composition by
118 favouring certain autotrophic groups over others, thereby exerting differential selection, as
119 shown in a study where cyanobacteria proportions in biofilm decreased under ALAN
120 (Grubisic et al., 2017).

121

122 The objectives of this study were to determine (1) the individual and combined effects of
123 urban stressors (BAC 12 and continuous light) on autotrophic organisms within the biofilm
124 (i.e. photosynthetic efficiency and lipid composition), and (2) the impact of these two
125 stressors on the taxonomic composition of the biofilm and the consequences for the
126 proportion of essential fatty acids, which could result in a decrease in the nutritional value of
127 this basal resource.

128

129

130

131

132

133

134

135

136

137 **2- Material and methods**

138 **2.1- Experimental design**

139 Biofilms were grown in a small pond in Cestas, near Bordeaux, France. Glass slides were
140 immersed at a depth of 30-50 cm for a colonization period of five months (December 2020
141 to April 2021). A previous study classified this small water body as a hypereutrophic pond
142 (Chaumet et al., 2019; Neury-Ormanni et al., 2020). At the end of the colonization period,
143 the glass slides covered by mature biofilms were randomly distributed among four series of

144 Experimental Units (EU) for the trial. The EUs consisted of aquaria of about 30 L filled with
145 pond water previously filtered (20 μm) to remove suspended material and most planktonic
146 organisms. The slides were divided among three parallel channels per EU, connected to 10-L
147 tanks. In each channel, 12 colonized glass slides were placed for subsequent exposure of the
148 biofilms to the different treatments (BAC 12 and ALAN). Biofilms corresponding to the day 0
149 (d0) sample were collected immediately after their recovery from the pond.

150 On d0, two EUs were contaminated with a solution of dodecylbenzyltrimethylammonium
151 chloride (BAC 12; Sigma Aldrich, France; CAS: 139-07-1, purity: >99%) to reach a
152 concentration of 30 mg.L^{-1} . This concentration had been found to be the EC_{50} for biofilm
153 photosynthesis inhibition in a preliminary toxicity experiment to assess BAC 12 toxicity
154 towards pond biofilm (see Appendix A). Light (20 $\mu\text{mol.s}^{-1}.\text{m}^{-2}$) was kept on overnight and
155 then from day 1 (d1), one control series and one BAC 12 series were exposed to an
156 alternating 14 h day / 10 h night photoperiod (alternated photoperiod, AP) and the other
157 two series (one control, one BAC 12) were exposed to a 24 h day photoperiod (continuous
158 photoperiod, CP) throughout the course of the experiment. Room temperature was
159 maintained constant at $20.5 \pm 0.1^{\circ}\text{C}$, while water temperature was kept at $18.7 \pm 0.2^{\circ}\text{C}$. The
160 tanks were refilled with 3 L of filtered pond water contaminated at 30 mg.L^{-1} BAC12 on day 4
161 (d4) to compensate for water evaporation.

162 2.2- Water chemistry measurements

163 On d0, d1, d2, d4, d7 and d10, 20 mL water samples were taken from all channels, filtered on
164 1- μm PTFE filters and stored at 4°C in the dark until analysis (performed within 48 h of
165 collection). Nutrients and mineral salts were analysed using a Metrohm 881 Compact Ionic
166 Chromatograph pro (Metrohm). Anion analysis (PO_4^- , NO_3^- , NO_2^- , Cl^- and SO_4^{2-}) was performed
167 using a Supp 4/5 Guard/4.0 precolumn followed by a Metrosep A Supp5 – 250/4.0 column.
168 The mobile phase was a mixture of a solution of 3.2 mmol.L^{-1} Na_2CO_3 and a solution of 1
169 mmol.L^{-1} NaHCO_3 . Cation analysis (Na^+ , K^+ , Ca^{2+} , Mg^{2+} and NH_4^+) was performed using a C4
170 Guard/4.0 precolumn followed by a Metrosep C6 - 250/4.0 column). All precolumns and
171 columns come from the provider Metrohm. The eluent used was a mixture of 2.5 mmol.L^{-1}
172 HNO_3 and a solution of 1.7 mmol.L^{-1} 10,12-Pentacosadynoic acid (PCDA). The limits of
173 quantification of the different ions analysed are shown in Table 1.

174 BAC 12 concentrations in the water were monitored frequently over the experiment, at d0,
175 d1, d2, d4, d7 and d10. Three samples of 20 mL were collected from each channel and stored
176 at -20°C together with the stock solution until analysis. The samples were analysed using an
177 Ultimate 3000 HPLC coupled with an API 2000 triple quadrupole mass spectrometer. We
178 used a Gemini® NX-C18 column from Phenomenex as a stationary phase. The mobile phase
179 was 90:10 5 mM ammonium acetate/acetonitrile. We worked in isocratic mode, so the
180 composition of the mobile phase was constant during the analysis. The flow rate was set at
181 0.6 mL.min^{-1} and the injection volume was set at 20 μL . An internal standard of benzyl-
182 2,3,4,5,6-d5-dimethyl-n-dodecylammonium chloride was used (Cluzeau, France; CAS: 139-
183 07-1, purity: >98%). Samples were diluted and the calibration range was from 1 to 200 $\mu\text{g.L}^{-1}$.
184 Quality controls were regularly injected at concentrations of 5 and 25 $\mu\text{g.L}^{-1}$, as well as
185 analytical blanks.

186

187 **2.3- Biofilm biological endpoints**

188 ***Photosynthetic efficiency***

189 We sampled 2 cm² of biofilm from three different glass slides for each treatment on d0, d2,
190 d4, d7, and d10, corresponding to three pseudoreplicates per treatment per sampling. Each
191 biofilm sample was then suspended in 3 mL of channel water. Photosynthetic efficiency was
192 assessed within one hour after collection using pulse amplification modulation equipment
193 (Phyto-PAM) from Heinz Walz GmbH. After these photosynthesis measurements, samples
194 were preserved for further microscopic analyses by adding a few drops of Lugol solution
195 then stored in the dark at 4°C.

196 ***Microscopic analyses***

197 For microscopic observations, a Nageotte counting slide (Marienfeld, Germany) was used
198 with 125 µL biofilm suspension samples collected on d0, d2 and d10. Observations were
199 made at x400 magnification under an optical microscope (Olympus BX51) equipped with a
200 digital camera. Ten fields of view were scanned for enumeration of diatoms, green algae,
201 cyanobacteria and micro-meiofauna (e.g. rotifers, ciliates, nematodes). Live (intact cell
202 content) and dead (empty frustules) diatoms were counted separately to estimate mortality
203 (Morin et al. 2010).

204 ***Lipid classes, bioconcentration and pigments***

205 Biofilms were scraped from glass slides on d0, d1, d2 and d10 (4 slides per treatment) and
206 were frozen in liquid nitrogen to prevent lipid degradation. The samples were then
207 lyophilized for 24 hours. Lipids were extracted using a mixture of MTBE-methanol (3:1 %v/v)
208 and UPW-methanol (3:1 %v/v) with 150 mg of microbeads. Biofilm cells (20 mg dry weight)
209 were then homogenized by agitating the samples with FastPrep. The upper organic fraction
210 of the samples (i.e. MTBE) was recovered by centrifugation, while the lower hydrophilic
211 fraction (mixture of UPW and methanol) was used to determine BAC 12 bioaccumulation.
212 For lipid analysis, samples were evaporated and injection solvent was added before analysis
213 by HPLC-MS/MS. Different stationary and mobile phases were used for the analysis of
214 phospholipids/glycolipids and triglycerides. For the phospholipid and glycolipid analyses, a
215 LUNA[®] NH₂ column (100 x 2 mm, 3 µm) from Phenomenex was used as the stationary
216 phase, and a mixture of acetonitrile and 40 mM ammonium acetate buffer as the mobile
217 phase. The flow rate was set at 400 µL.min⁻¹. The proportions of these two solutions are
218 given in Appendix D. For the analysis of triglycerides and betaine lipids (i.e.
219 diacylglyceryltrimethylhomo-Ser, DGTS), a KINETEX[®] C8 column (100 x 2.1 mm, 2.6 µm) from
220 Phenomenex was used as the stationary phase, and the mobile phase was a mix of a solution
221 of acetonitrile/water/40 mM ammonium acetate buffer (600/390/10, v/v/v) and a solution
222 of isopropanol/acetonitrile/1 M ammonium acetate buffer (900/90/10, v/v/v). The flow rate
223 was set at 300 µL.min⁻¹. The proportions of these two solutions are given in Appendix D.
224 Results were then pre-treated with ANALYST[®] 1.6.2 software from Sciex. For polar lipids (i.e.
225 glycolipids and phospholipids), the limits of quantification ranged from 0.1 to 0.5 nmol.mg⁻¹,

226 depending on the lipid classes. For triglycerides and DGTS, the limits of quantification
227 reached were 0.01 and 0.1 nmol.mg⁻¹, respectively. Results were expressed as nmol.g⁻¹
228 freeze-dried biofilm.

229 The same analytical method used for water samples was used to determine bioaccumulated
230 BAC 12 in the hydrophilic fraction of the previously extracted biofilm. It was generally
231 necessary to perform significant dilutions (i.e. 10,000-fold) in order to stay within the
232 calibration range. Results were then expressed in the log₁₀ value of the bioaccumulation
233 factor (i.e. log(BCF)). The bioaccumulation factor (BCF) was calculated according to the
234 following formula:

$$235 \quad BCF = \frac{\text{Concentration of BAC 12 in biofilm (mg/kg)}}{\text{Concentration of BAC 12 in water (mg/L)}}$$

236 On selected freeze-dried samples, pigment analyses were also performed (see Appendix C).
237 Ten mg of dry biofilm were put in solution using 10 mL of acetone. After 20 minutes of
238 ultrasonication, the mix was filtered on a Büchner filter to remove the solid phase.
239 Absorption was measured at the wavelengths 630 nm, 647 nm, 664 nm, 665 nm and 750 nm
240 and was then remeasured at the same wavelengths after acidification of the samples. The
241 concentrations of chlorophyll pigments and phaeopigments were determined following the
242 equations of Lorenzen (Lorenzen, 1967).

243 **2.4- Data analyses**

244 Data were processed using R software (R Core Team, 2022). One- and two-way ANOVAs
245 were performed (after verification of homogeneity of variances) to assess the effect of light
246 on BAC 12 degradation and nutrient levels in the different treatments. Two-way ANOVAs
247 with repeated measures were applied to assess the effect of BAC 12 and ALAN on biofilm
248 endpoints. We also performed a principal component analysis to present a graphic
249 projection of the different fatty acid profiles.

250

251

252

253

254

255

256 **3- Results**
 257 **3.1- Water chemistry**

258 **Table 1. Principal ions and BAC 12 concentrations (mg.L⁻¹) in the four experimental treatments along the ten days exposure. Results are expressed as the mean and**
 259 **standard error for the whole experiment. Two-way Anovas were conducted with Light and BAC 12 as the two factors. BAC 12 = contaminated biofilm; CONTROL = non-**
 260 **exposed biofilm; AP = alternated photoperiod; CP = continuous photoperiod; LOQ = Limit of quantification.**
 261
 262

Treatment	BAC 12	NO ₂	NO ₃	PO ₄	SO ₄	Cl	NH ₄	Na	K	Ca	Mg
CONTROL-AP	<LOQ	0.02 ± 0.01	0.75 ± 0.22	0.03 ± 0.05	17.84 ± 0.68	33.0 ± 1.4	0.10 ± 0.13	18.78 ± 0.89	4.21 ± 0.25	49.5 ± 2.6	4.18 ± 0.20
BAC 12-AP	27 ± 12	0.02 ± 0.01	0.66 ± 0.38	0.03 ± 0.04	18.9 ± 1.8	35.5 ± 3.1	0.11 ± 0.12	19.7 ± 2.0	4.34 ± 0.45	52.2 ± 5.7	4.41 ± 0.45
CONTROL-CP	<LOQ	0.02 ± 0.01	1.35 ± 0.52	0.01 ± 0.01	17.53 ± 0.68	30.27 ± 0.79	0.09 ± 0.14	18.52 ± 0.74	4.12 ± 0.14	48.4 ± 1.5	4.09 ± 0.14
BAC 12-CP	17.2 ± 7.5	0.04 ± 0.06	1.69 ± 0.62	0.03 ± 0.04	21 ± 4	36.4 ± 6.0	0.09 ± 0.12	22.0 ± 4.4	4.80 ± 0.95	57.8 ± 11.5	4.90 ± 0.95
LOQ	0.001	0.005	0.01	0.01	0.005	0.01	0.005	0.01	0.0025	0.15	0.15
Significant factor(s) and interaction(s)	Light	None	BAC 12	NA	BAC 12	BAC 12	NA	BAC 12	NA	BAC 12	BAC 12
p value	2.97e-08	>0.05	3.0e-4	NA	0.026	0.007	NA	0.040	NA	0.035	0.030

263

264 In the control channels, BAC 12 concentrations were always below detection limit
265 (Table 1), confirming that no cross-contamination occurred. Contaminant concentrations
266 averaged $27 \pm 12 \text{ mg.L}^{-1}$ (AP) and $17 \pm 7 \text{ mg.L}^{-1}$ (CP) in the BAC 12 treatments. Differences in
267 BAC 12 concentrations were observed between the BAC 12 treatment channels exposed to
268 an alternated photoperiod and those exposed to a continuous photoperiod ($F_{[1,10]} = 232.72$; p
269 $= 2.97\text{e-}08$), suggesting that degradation occurred under the continuous photoperiod.
270 Nutrient concentrations were also modified by BAC 12 exposure (Table 1). Indeed, BAC 12
271 addition (indirectly via effects on organism) resulted in higher concentrations of NO_3 , SO_4 , Cl ,
272 Na^+ , Ca^{2+} and Mg^+ than in the control (Table 4) while light exposed solutions show no effects
273 on nutrient concentrations.

274 .

275

276

277

278

279

280

281

282

283

284

285

286

287

288

289

290

291

292

293

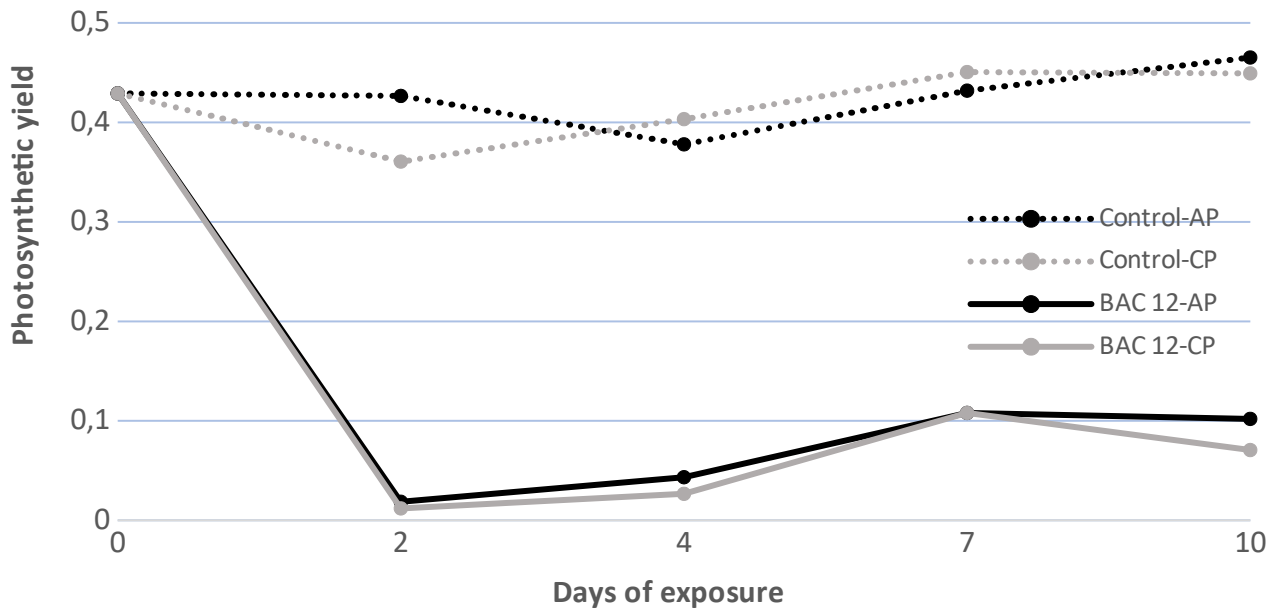
294

295 **3.2- Effects of BAC12 and ALAN on biofilm communities**

296

297 ***Effects of BAC 12 on photosynthetic efficiency***

298



299

300 **Figure 1. Evolution of photosynthesis yield in biofilms along the ten days of the experiment. BAC 12 =**
301 **contaminated biofilm; CTRL = non-exposed biofilm; AP = Alternated Photoperiod; CP =**
302 **Continuous Photoperiod**

303

304 Figure 1 shows that photosynthetic activity was stable over the experiment, with a mean
305 value of 0.42 ± 0.01 in the control channels, regardless of the light exposure treatment ($F_{[1,42]} = 2.65$;
306 $p > 0.05$). Biofilms exposed to BAC 12 showed an almost complete inhibition of
307 photosynthetic yield starting from d2 and lasting until the end of the experiment ($F_{[1,42]} =$
308 1279 ; $p = 4.45e33$). In the same way as for control channels, photosynthetic activity showed
309 no difference between the two light conditions for contaminated channels ($F_{[1,42]} = 0.18$; $p =$
310 0.67).

311 **Effects on community composition**

Table 2. Evolution of the taxonomic composition of biofilms during the experiment. Densities are expressed as individuals $\times 10^3$ / cm², i.e. number of cells for microalgae, and number of organisms for microfauna. Diatom mortality is expressed in %. BAC 12 = contaminated biofilm; CTRL = non-exposed biofilm; AP = Alternated Photoperiod; CP = Continuous Photoperiod

312

Date	Treatment	Diatom density	Diatom mortality	Green algae density	Cyanobacteria density	Microfauna density
d0	Control	21.5 ± 5.5	7 ± 6	1.8 ± 1.2	3.2 ± 3.2	0.19 ± 0.05
d2	Control-AP	94.2 ± 8.6	3 ± 3	17.8 ± 4.1	1.1 ± 0.2	0.4 ± 0.2
d2	BAC 12-AP	75.5 ± 10.8	3 ± 3	7.9 ± 2.6	0	0.2 ± 0.2
d2	Control-CP	88.0 ± 6.5	3 ± 3	34.5 ± 43.4	0	0.2 ± 0.2
d2	BAC 12-CP	96.7 ± 24.6	2 ± 2	4.2 ± 1.6	0	0
d10	Control-AP	65.5 ± 11.0	5 ± 5	150.4 ± 125.8	7.5 ± 7.4	0.6 ± 0.5
d10	BAC 12-AP	85.7 ± 24.6	2 ± 2	12.6 ± 13.9	3.2 ± 3.2	0
d10	Control-CP	60.9 ± 13.4	6 ± 6	236.1 ± 78.	0	0.6 ± 0.2
d10	BAC 12-CP	67.3 ± 25.4	1 ± 1	20.5 ± 7.7	0	0
Significant factor(s) and interaction(s)		None	BAC 12	BAC 12 × Time	None	BAC 12 × Time
p-value		>0.05	0.031	9.53e-05	>0.05	0.003

313 Diatoms (91%) dominated the biofilm community at d0 and low proportions of green algae
314 (5%), cyanobacteria (4%) and microfauna (1%) were observed (Table 2). In the control
315 channels, green algae developed markedly and became the main algal group in terms of
316 density by d10, with no significant effect of the photoperiod conditions (e.g. 67% in
317 channels exposed to an alternated photoperiod and 79% in those exposed to a continuous
318 photoperiod). There was also an increase in proportions of green algae in the BAC 12
319 contaminated channels, although this was not as marked as in the control channels
320 (significant Date × BAC interaction; Table 2). Microfauna numbers increased in control
321 channels, but had completely disappeared from biofilms exposed to BAC 12 by d10
322 (significant Date × BAC interaction; Table 2). Light conditions did not have a significant
323 impact on the biofilm taxonomic composition.

324 Diatom mortality (based on the ratio between frustules without cell content and total cell
325 numbers) showed a significant effect of BAC 12 exposure in the AP and CP treatments (Table
326 2). Note that microscopic observations highlighted differences in the aspect (shape, colour)
327 of chloroplasts in diatoms and chlorophytes exposed to BAC 12, becoming highly granular
328 and darker (Figure B.2). These were, however, not considered as 'dead' cells in estimating
329 diatom mortality.

330

331

332

333

334

335

336

337

338

339

340

341

342

343

344

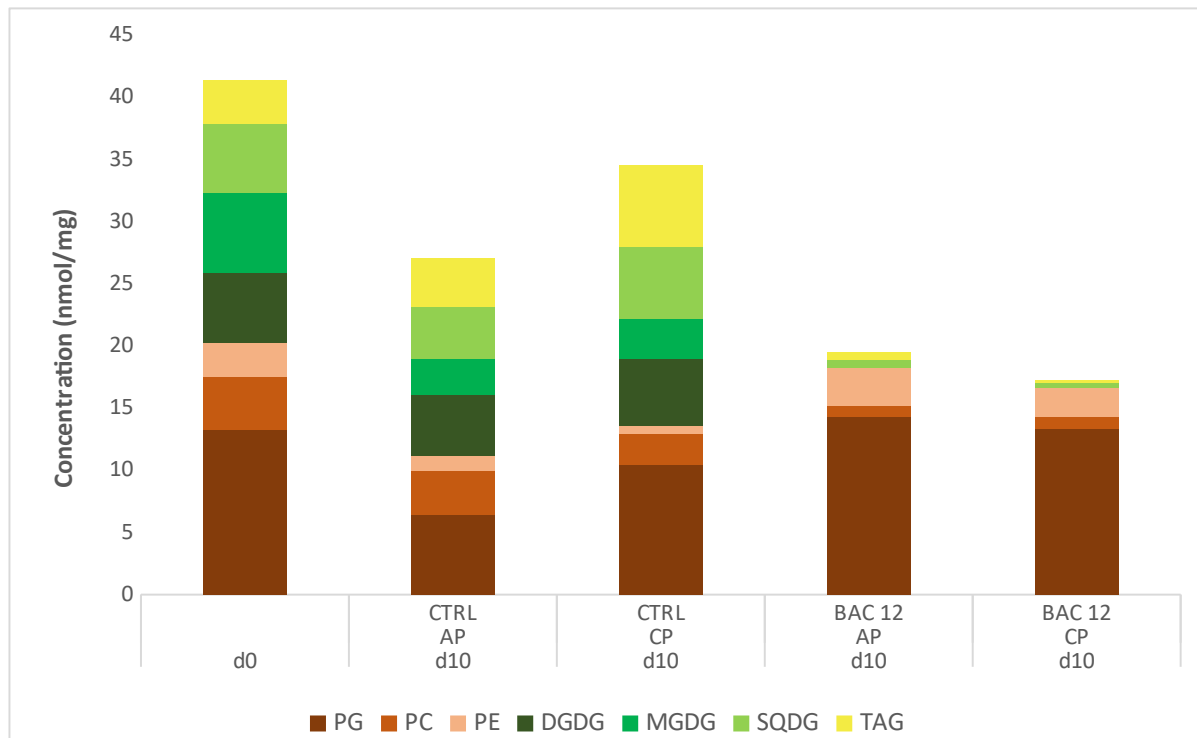
345

346

347

348 3.3- Impacts of BAC 12 and continuous photoperiod on polar lipids

349



350
351

352 **Figure 2. Effects of BAC 12 and continuous photoperiod on the proportion of total lipids and on lipid classes.**
 353 **BAC 12 = contaminated biofilm; CTRL = non-exposed biofilm; AP = alternated photoperiod; CP = continuous**
 354 **photoperiod; PE = phosphatidylethanolamine; PC = phosphatidylcholine; PG = phosphatidylglycerol; DGDG =**
 355 **digalactosyldiacylglycerol; MGDG = monogalactosyldiacylglycerol; SQDG = sulfoquinovosyldiacylglycerol;**
 356 **TAG = triacylglycerides.**

357

358 On d0, total lipid concentration reached $42.6 \text{ nmol.mg}^{-1}$ of freeze-dried biofilm. Almost half
 359 of the lipids were phospholipids, and the other half were glycolipids, while neutral lipids
 360 (TAG) represented a minor portion (Table 3). By d10, total lipid concentration had decreased
 361 in all treatments down to an average of $23.6 \pm 7.53 \text{ nmol.mg}^{-1}$ of freeze-dried biofilm (Table
 362 3). No significant differences were found between light conditions, while BAC significantly
 363 affected glycolipids. As an example, Figure 2 shows lipid profiles under BAC12 exposure and
 364 alternated photoperiod on d0 and d10. At the beginning of the experiment,
 365 phosphatidylglycerol (PG) was the predominant lipid in the biofilms, although phospholipids
 366 and glycolipids in the biofilms were evenly distributed. Although total lipids decreased over
 367 time in the controls, the proportions of phospholipids and glycolipids remained similar to
 368 those at d0, all the main classes of lipids present. In the samples exposed to BAC 12,
 369 glycolipids such as monogalactosyldiacylglycerol (MGDG) and digalactosyldiacylglycerol
 370 (DGDG) decreased significantly, or even became barely detectable. Phospholipids, especially
 371 PE and phosphatidylglycerol (PG) were higher in biofilms exposed to BAC 12 compared to
 372 control (Figure 2, Table 3). Diacylglyceryltrimethylhomo-Ser (DGTS) was never detected and,
 373 therefore, is not mentioned further.

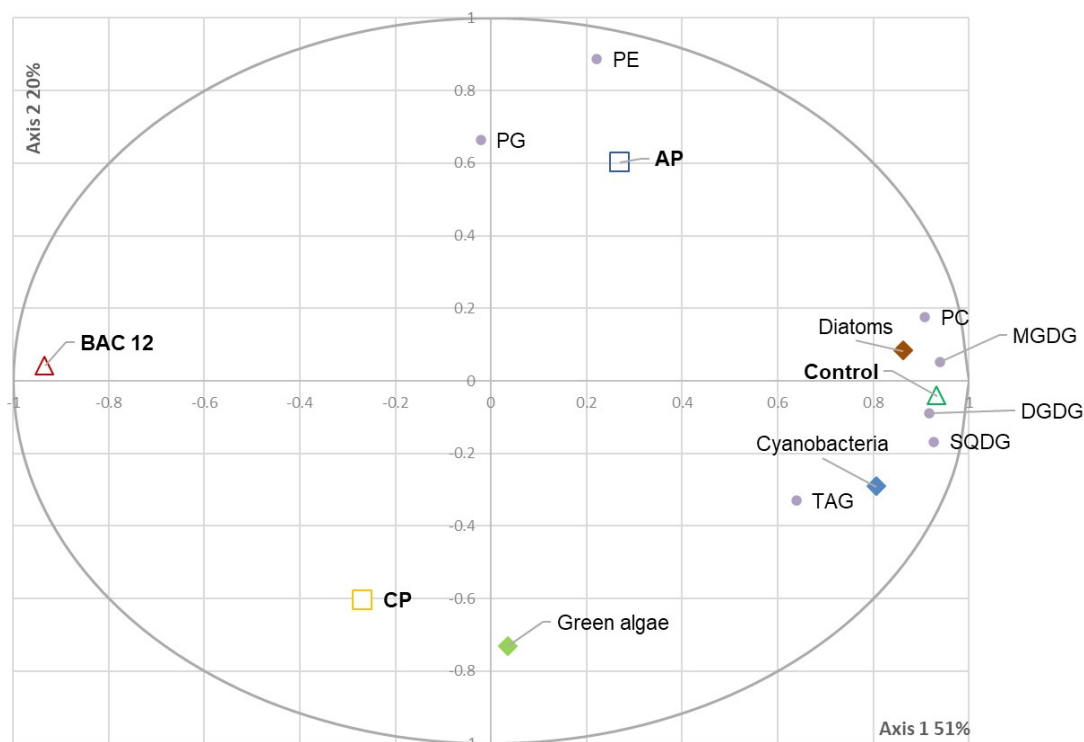
Table 3: Evolution of lipid content of biofilms (in nmol.g⁻¹ freeze-dried biofilm) between the beginning and the end of the experiment. BAC 12 = contaminated biofilm; CTRL = non-exposed biofilm; AP = Alternated Photoperiod; CP = Continuous Photoperiod. Two-ways ANOVA on repeated measure was applied on data.

Date	Treatment	Neutral lipids (TAG)	PG	PE	PC	MGDG	DGDG	SQDG	Σ Phospholipids	Σ Glycolipids	Total lipids
d0	Control	4.2 ± 2.5	13.7 ± 3.1	2.8 ± 0.5	4.6 ± 0.2	6.4 ± 1.6	5.6 ± 1.2	5.3 ± 1.1	21.0 ± 3.3	17.3 ± 2.4	42.6 ± 3.2
d10	Control-AP	3.9 ± 2.0	6.4 ± 1.0	1.3 ± 0.5	3.5 ± 1.5	2.9 ± 0.5	4.8 ± 0.8	4.2 ± 0.7	11.2 ± 2.4	12.0 ± 0.4	27.1 ± 4.1
d10	BAC 12-AP	0.2 ± 0.3	14.3 ± 2.6	3.0 ± 0.4	0.9 ± 0.4	0	0	0.7 ± 0.2	18.2 ± 2.6	0.7 ± 0.2	19.1 ± 2.6
d10	Control-CP	6.6 ± 2.9	6.9 ± 6.7	0.7 ± 0.1	2.6 ± 1.1	3.3 ± 1.1	5.3 ± 0.2	5.8 ± 1.2	10.1 ± 7.8	14.4 ± 2.2	31.1 ± 8.1
d10	BAC 12-CP	0.1 ± 0.1	13.3 ± 3.5	2.3 ± 1.0	1.0 ± 1.0	0	0	0.4 ± 0.2	16.6 ± 5.2	0.4 ± 0.2	17.1 ± 5.3
	Significant factor(s)	BAC 12 × Time	BAC 12× Time	BAC 12× Time	BAC 12× Time	BAC 12× Time	BAC 12× Time	BAC 12× Time	None	BAC 12× Time	BAC 12× Time
	p-value	0.01	0.019	0.002	0.006	0.006	1.22e-06	2.16e-05	>0.05	3.46e-07	8.00e-03

376

377 3.4- Relationships between taxonomic data and lipid profiles

378



379

380

381

382 **Figure 3: Principal component analysis conducted on lipid and taxonomic data at d0, d1, d2 and d10.**

383 **BAC 12 = contaminated biofilm; AP = alternated photoperiod CP = continuous photoperiod; PE =**

384 **phosphatidylethanolamine; PC = phosphatidylcholine; PG = phosphatidylglycerol; DGDG =**

385 **digalactosyldiacylglycerol; MGDG = monogalactosyldiacylglycerol; SQDG = sulfoquinovosyldiacylglycerol;**

386 **TAG = triacylglycerides.**

387

388 The principal component analysis (Figure 3) illustrates the relationships between the
389 different lipid classes, the three taxonomic groups present in the biofilms and the two
390 stressors (light and BAC 12). Axis 1 explains 51% of the total variance and shows an
391 anticorrelation between the presence of the three classes of glycolipids (i.e. SQDG, DGDG
392 and MGDG) and BAC 12 exposure. Diatom and cyanobacteria densities are also negatively
393 correlated with BAC 12 exposure and positively correlated with glycolipids. Both TAG and PC
394 cluster with diatoms. The second axis explains 20% of the total variance and shows how
395 higher densities of green algae are associated with continuous light. PE and PG, associated
396 with axis 2, are not specific and can also be found in bacteria, which were not considered in
397 this study.

398

399

400

401

402 3.5- BAC 12 bioaccumulation in biofilms

403

404

405 **Table 4. Evolution of BAC 12 bioaccumulated in biofilms (expressed in log(BCF)) between the different**
406 **photoperiod treatments for the hydrophilic fraction of lipidomic samples only. AP = alternated photoperiod**
407 **CP = continuous photoperiod**

408

	d1	d2	d10
AP	2.18 ± 1.70	3.03 ± 0.34	3.40 ± 0.10
CP	3.23 ± 0.30	2.90 ± 0.98	3.33 ± 0.10

409

410 Table 4 shows the log(BCF) for the hydrophilic fraction at d1, d2 and d10 for the two
411 photoperiod conditions. BAC 12 was recovered from biofilms for every treatment and every
412 sampling time, showing that this compound bioaccumulates well in algal biofilms, with a
413 mean log(BCF) of 3.22 ± 0.25. The amount of BAC 12 bioaccumulated in the biofilms showed
414 no significant difference between sampling dates ($F_{[2,28]} = 2.38$; $p = 0.11$) and no significant
415 difference in bioaccumulation was found between the two photoperiod treatments ($F_{[1,28]} =$
416 0.28 ; $p = 0.60$). Overall, the amount of BAC 12 bioaccumulated in biofilms was stable through
417 the experiment with no significant difference was found between the two photoperiod
418 treatments ($F_{[2,28]} = 0.025$; $p = 0.98$)

419

420 4. Discussion

421 4.1- Experimental conditions and contamination

422 BAC 12 seemed to have an indirect effect on nutrient concentrations over the 10-day
423 exposure period of our experiment, possibly by affecting biofilm microorganisms (reduced
424 growth). BAC 12 concentrations in the channels under the continuous photoperiod
425 significantly decreased over time. This could be the result of photodegradation of the
426 contaminant. A previous study showed that freshwater biofilms can improve the
427 photodegradation of organic contaminants by being a source of reactive oxygen species
428 (ROS) such as hydroxyl (OH·) or superoxide (O₂⁻) radicals (Yin et al. 2022). Contrary to the
429 hypothesis of Pozo-Antonio and Sanmartin (2018), who suggested that artificial light could
430 lead to an increase in internalization of the contaminant, we found no significant difference
431 in BAC12 concentrations in biofilm between the different light conditions (Table 2). Thus, our
432 results do not support the hypothesis of a higher uptake of the substance from the water
433 through increased bioaccumulation under continuous light exposure. This lower
434 concentration might be linked to some bacterial strains such as *Aeromonas hydrophila* that
435 can biodegrade BAC 12 and use the degradation product as an energy source (Patrauchan

436 and Oriel, 2003). However, resistant strains cannot withstand BAC 12 concentrations higher
437 than 10 mg.L⁻¹ (Kreuzinger et al., 2007).

438 **4.2- Effects of BAC 12 on the biofilm**

439 The first effect of BAC 12 observed was the marked and rapid decrease in photosynthetic
440 efficiency (more than 90% compared with the initial yield; Figure 1). This sudden inhibition of
441 photosynthesis was not expected because the exposure concentration was based on the EC₅
442 for photosynthesis inhibition after 4 hours of exposure determined in a preliminary
443 experiment (EC₅ = 30 mg.L⁻¹; Figure A).

444 Based on our microscopic observations, diatom mortality was low in our samples (<10%) and
445 not significantly different from the controls. It should be noted that only diatoms that no
446 longer had chlorophyll in their cell content (Morin et al. 2010) were considered as dead cells
447 in our study, while cells with chloroplasts were counted as live diatoms. However, many of
448 the cells where content was observed nevertheless seemed to have suffered critical
449 alteration of their photosynthetic equipment (Figure B.2). Their integrity was potentially
450 severely affected, which could explain the loss of photosynthetic yield in biofilms exposed to
451 BAC 12. This deterioration of cell integrity may be due to the fact that BAC 12 is able to
452 quickly penetrate the cell (Severina et al. 2001).

453 The striking decrease in lipid content in biofilms exposed to BAC 12, particularly glycolipids
454 found mainly in thylakoid membranes within photosynthetic cells (Zulu et al., 2018),
455 supports the idea that the contaminant is internalized within cells. The degradation of the
456 photosynthetic material observed microscopically (Figure B.2) in turn explains the alteration
457 of photosynthesis. In parallel to this decrease in glycolipids with BAC 12 contamination, we
458 observed an increase in phospholipids. It is difficult to clearly explain this increase because
459 the phospholipid groups analysed (i.e. PE, PC and PG) are not specific to any taxonomic
460 group and can be found in both the plasma membranes of microalgae (Zulu et al., 2018) and
461 in prokaryotic cells (Li-Beisson et al., 2013). One hypothesis to explain this increase could be
462 the development of BAC 12-resistant bacteria. Indeed, the mechanism of resistance to
463 benzalkonium chloride identified in *Pseudomonas aeruginosa* consists of an increase in the
464 percentage of phospholipids (Sakagami et al. 1989).

465 Sensitivity to BAC 12 differed among algal taxa, whose proportions changed over time, and
466 with BAC 12 concentration. This result suggests that the biofilm community acclimated to
467 the chemical stress and that only resistant/tolerant species survived BAC 12 exposure.
468 Diatoms appeared to be minimally affected based on growth and mortality, even though
469 their photosynthetic structure and cell content was altered (Figure B.2). Green algae, which
470 experienced rapid growth in non-contaminated channels, appeared to be negatively affected
471 by BAC 12 at d10. BAC 12 also had a strong effect on heterotrophic microfauna naturally
472 present in the biofilms (e.g. rotifers, tardigrades), suggesting that they are highly sensitive to
473 this contaminant.

474

475

476

477

478 **4.3- Effects of ALAN on the biofilm**

479 The continuous photoperiod did not significantly modify the structure or physiology of the
480 autotrophic organisms in the biofilm based on the parameters that we investigated.
481 Although the continuous photoperiod did not result in growth differences among diatoms,
482 green algae and cyanobacteria, the ordination (Figure 3) suggests that ALAN could benefit
483 green algae, as already demonstrated in some previous studies (Yang et al., 2012; Ugwu et
484 al., 2007).

485

486 It would also be of interest to perform more in-depth lipid analysis to determine whether
487 fatty acids show a clearer difference between light conditions than was visible from a global
488 assessment of lipid classes. Amini Khoeyi et al. (2011), studying *Chlorella vulgaris*, showed
489 that a prolonged photoperiod can decrease microalgal content of monounsaturated (MUFA)
490 and polyunsaturated (PUFA) fatty acids. Such a decrease could be enhanced by BAC 12
491 activity, which can disrupt lipid membranes and degrade lipids, thereby
492 possibly exacerbating the negative effect of the prolonged photoperiod on MUFA and PUFA
493 content. A decrease in essential polyunsaturated fatty acids, such as certain omega-3 and
494 omega-6 types, could alter the nutritional quality of biofilms and decrease the energy supply
495 along the trophic chain (Brett and Müller-Navarra; 1997). Concerning the polar lipid classes,
496 an increase of MGDG or DGDG is often observed during low light intensity exposures
497 (Gushina and Harwood, 2009). In the present experiment, while the light intensity remained
498 the same, the duration of exposure varied, which could explain the absence of a significant
499 effect on these two glycolipids over time. Conversely, high light levels can lead to a decrease
500 in polar lipids, especially phospholipids, in favour of TAGs, especially in the case of
501 filamentous green algae such as *Cladophora* spp. Such a phenomenon was not clearly
502 observed here, which could be due to compensation phenomena or to our averaging of the
503 lipid mixture across different organisms present within a natural biofilm, which differs from
504 the analysis of an isolated chlorophyte strain.

505

506

507 **4.4- Combined effects of BAC and ALAN on the biofilm**

508 Contrary to our hypotheses, BAC 12 and ALAN exposure did not show interaction effects on
509 any of the parameters monitored in this experiment. However, continuous light impacted
510 the fate of BAC 12 by decreasing exposure concentrations in the medium. As the high
511 concentration of BAC 12 tested drove most of the changes observed in biofilm composition
512 and physiology, we cannot exclude that BAC 12 exposure masked possible interactions
513 between the stressors. Further experiments combining lower concentrations of BAC 12 with
514 ALAN would be required to completely rule out any interaction effects on aquatic biofilms.

515

516

517

518
519
520
521
522
523
524
525
526
527
528
529
530
531
532
533
534
535
536
537
538
539
540
541
542
543
544
545
546
547
548
549
550
551
552
553
554
555
556
557
558
559
560

5- Conclusion

In this experiment, we demonstrated that BAC 12 exposure strongly impacts biofilms. The damage to the quality and quantity of photosynthetic pigments following BAC 12 exposure implies a serious impact on the photosynthetic efficiency of the biofilm. There was also evidence for an impact on the structure of the biofilm as changes in its taxonomic composition were observed. Indeed, even though the mortality index did not show greater mortality in the exposed diatoms compared with the controls, microscopic observations suggest that a marked number of individuals were strongly impacted on a physiological level (degraded cell content) and were potentially not viable. This hypothesis is supported by the results obtained during the lipidomic analysis, highlighting a strong decrease in the lipid classes associated with thylakoid membranes specific to microalgae.

In contrast, ALAN did not lead to any significant change in biofilms, even though the ALAN conditions modified their exposure to BAC 12. In view of the increased use of BAC 12 in the context of the Covid-19 pandemic and the likely increase in its concentration in urban waters (downstream of WWTPs) where ALAN is often common, it would also be necessary to investigate whether the effects identified in the present study are manifested at environmental concentrations in order to reassess the risk posed by BAC 12 to aquatic biodiversity.

Aknowledgements

The authors aknowledge the financial support from the Institut National de Recherche pour l’Agriculture, l’alimentation et l’Environnement (INRAE), l’Institut National de la Recherche Scientifique (INRS) and the Groupe de Recherche Interuniversitaire en Limnologie (GRIL).

561
562
563
564

565 **References**

566

- 567 Abbott, T., Kor-Bicakci, G., Islam, M.S., Eskicioglu, C., 2020. A Review on the Fate of Legacy and
568 Alternative Antimicrobials and Their Metabolites during Wastewater and Sludge Treatment.
569 International Journal of Molecular Sciences 21, 9241. <https://doi.org/10.3390/ijms21239241>
- 570 Mini Khoeyi, Z., Seyfabadi, J., Ramezanzpour, Z., 2012. Effect of light intensity and photoperiod
571 on biomass and fatty acid composition of the microalgae, *Chlorella vulgaris*. *Aquacult Int* 20,
572 41–49. <https://doi.org/10.1007/s10499-011-9440-1>
- 573 Brett, M., Müller-Navarra, D., 1997. The role of highly unsaturated fatty acids in aquatic foodweb
574 processes. *Freshwater Biology* 38, 483–499. [https://doi.org/10.1046/j.1365-](https://doi.org/10.1046/j.1365-2427.1997.00220.x)
575 [2427.1997.00220.x](https://doi.org/10.1046/j.1365-2427.1997.00220.x)
- 576 Chaumet, B., Morin, S., Hourtané, O., Artigas, J., Delest, B., Eon, M., Mazzella, N., 2019. Flow
577 conditions influence diuron toxicokinetics and toxicodynamics in freshwater biofilms.
578 *Science of The Total Environment* 652, 1242–1251.
579 <https://doi.org/10.1016/j.scitotenv.2018.10.265>
- 580 Chen, Y., Geurts, M., Sjollema, S.B., Kramer, N.I., Hermens, J.L.M., Droge, S.T.J., 2014. Acute
581 toxicity of the cationic surfactant C12-benzalkonium in different bioassays: How test design
582 affects bioavailability and effect concentrations. *Environmental Toxicology and Chemistry* 33,
583 606–615. <https://doi.org/10.1002/etc.2465>
- 584 Gara, M., Scharf, S., Scheffknecht, C., Gans, O., 2007. Occurrence of selected surfactants in
585 untreated and treated sewage. *Water Research* 41, 4339–4348.
586 <https://doi.org/10.1016/j.watres.2007.06.027>
- 587 Demailly, F., Elfeky, I., Malbezin, L., Le Guédard, M., Eon, M., Bessoule, J.-J., Feurtet-Mazel, A.,
588 Delmas, F., Mazzella, N., Gonzalez, P., Morin, S., 2019. Impact of diuron and S-metolachlor
589 on the freshwater diatom *Gomphonema gracile*: Complementarity between fatty acid
590 profiles and different kinds of ecotoxicological impact-endpoints. *Science of The Total*
591 *Environment* 688, 960–969. <https://doi.org/10.1016/j.scitotenv.2019.06.347>
- 592 Eich, J., Dürholt, H., Steger-Hartmann, T., Wagner, E., 2000. Specific Detection of Membrane-Toxic
593 Substances with a Conductivity Assay. *Ecotoxicology and Environmental Safety* 45, 228–235.
594 <https://doi.org/10.1006/eesa.1999.1854>
- 595 Falchi, F., Cinzano, P., Duriscoe, D., Kyba, C.C.M., Elvidge, C.D., Baugh, K., Portnov, B.A.,
596 Rybnikova, N.A., Furgoni, R., n.d. The new world atlas of artificial night sky brightness.
597 *Science Advances* 2, e1600377. <https://doi.org/10.1126/sciadv.1600377>
- 598 Rubisic, M., Singer, G., Bruno, M.C., Grunsvan, R.H.A. van, Manfrin, A., Monaghan, M.T., Hölker,
599 F., 2017. Artificial light at night decreases biomass and alters community composition of
600 benthic primary producers in a sub-alpine stream. *Limnology and Oceanography* 62, 2799–
601 2810. <https://doi.org/10.1002/lno.10607>
- 602 Kreuzinger, N., Fuerhacker, M., Grillitsch, B., Scharf, S., Uhl, M., Gans, O., 2007. Methodological
603 approach towards the environmental significance of uncharacterized substances — quaternary
604 ammonium compounds as an example. *Desalination* 215, 209–222.
605 <https://doi.org/10.1016/j.desal.2006.10.036>

- 606 Patrauchan, M.A., Oriel, P.J., 2003. Degradation of benzyldimethylalkylammonium chloride by
607 *Aeromonas hydrophila* sp. K. J. Appl. Microbiol. 94, 266–272. <https://doi.org/10.1046/j.1365->
608 2672.2003.01829.x
- 609 Ehrilas, G.A., Blotevogel, J., Stewart, P.S., Borch, T., 2015. Biocides in Hydraulic Fracturing Fluids:
610 A Critical Review of Their Usage, Mobility, Degradation, and Toxicity. Environ. Sci. Technol.
611 49, 16–32. <https://doi.org/10.1021/es503724k>
- 612 Kim, M., Hatt, J.K., Weigand, M.R., Krishnan, R., Pavlostathis, S.G., Konstantinidis, K.T., 2018.
613 Genomic and Transcriptomic Insights into How Bacteria Withstand High Concentrations of
614 Benzalkonium Chloride Biocides. Appl. Environ. Microbiol. 84.
615 <https://doi.org/10.1128/AEM.00197-18>
- 616 Kreuzinger, N., Fuerhacker, M., Scharf, S., Uhl, M., Gans, O., Grillitsch, B., 2007. Methodological
617 approach towards the environmental significance of uncharacterized substances —
618 quaternary ammonium compounds as an example. Desalination 215, 209–222.
619 <https://doi.org/10.1016/j.desal.2006.10.036>
- 620 Zimmerer, K., Eitel, A., Braun, U., Hubner, P., Daschner, F., Mascart, G., Milandri, M., Reinthaler,
621 F., Verhoef, J., 1997. Analysis of benzalkonium chloride in the effluent from European
622 hospitals by solid-phase extraction and high-performance liquid chromatography with post-
623 column ion-pairing and fluorescence detection. Journal of Chromatography A 774, 281–286.
624 [https://doi.org/10.1016/S0021-9673\(97\)00242-2](https://doi.org/10.1016/S0021-9673(97)00242-2)
- 625 Avorgna, M., Russo, C., D’Abrosca, B., Parrella, A., Isidori, M., 2016. Toxicity and genotoxicity of
626 the quaternary ammonium compound benzalkonium chloride (BAC) using *Daphnia magna*
627 and *Ceriodaphnia dubia* as model systems. Environmental Pollution 210, 34–39.
628 <https://doi.org/10.1016/j.envpol.2015.11.042>
- 629 Gal, J.S., González, J.J., Kaiser, K.L.E., Palabrica, V.S., Comelles, F., García, M.T., 1994. On the
630 Toxicity and Biodegradation of Cationic Surfactants Über die Toxizität und den biologischen
631 Abbau kationischer Tenside. Acta hydrochimica et hydrobiologica 22, 13–18.
632 <https://doi.org/10.1002/aheh.19940220105>
- 633 Beisson, Y., Shorrosh, B., Beisson, F., Andersson, M.X., Arondel, V., Bates, P.D., Baud, S., Bird,
634 D., DeBono, A., Durrett, T.P., Franke, R.B., Graham, I.A., Katayama, K., Kelly, A.A., Larson, T.,
635 Markham, J.E., Miquel, M., Molina, I., Nishida, I., Rowland, O., Samuels, L., Schmid, K.M.,
636 Wada, H., Welti, R., Xu, C., Zallot, R., Ohlrogge, J., 2013. Acyl-Lipid Metabolism. arbo.j 2013.
637 <https://doi.org/10.1199/tab.0161>
- 638 Ingcore, T., Rich, C., 2004. Ecological light pollution. Frontiers in Ecology and the Environment 2,
639 191–198. [https://doi.org/10.1890/1540-9295\(2004\)002\[0191:ELP\]2.0.CO;2](https://doi.org/10.1890/1540-9295(2004)002[0191:ELP]2.0.CO;2)
- 640 Lorenzen, C.J., 1967. Determination of chlorophyll and pheo-pigments: Spectrophotometric
641 equations. Limnol. Oceanogr. 12, 343–346. <https://doi.org/10.4319/lo.1967.12.2.0343>
642
- 643 Maggi, E., Serôdio, J., 2020. Artificial Light at Night: A New Challenge in Microphytobenthos
644 Research. Front. Mar. Sci. 7. <https://doi.org/10.3389/fmars.2020.00329>
- 645 Martínez-Carballo, E., Sitka, A., González-Barreiro, C., Kreuzinger, N., Fürhacker, M., Scharf, S.,
646 Gans, O., 2007. Determination of selected quaternary ammonium compounds by liquid
647 chromatography with mass spectrometry. Part I. Application to surface, waste and indirect
648 discharge water samples in Austria. Environmental Pollution 145, 489–496.
649 <https://doi.org/10.1016/j.envpol.2006.04.033>
- 650 Morin, S., Proia, L., Ricart, M., Bonnineau, C., Geiszinger, A., Ricciardi, F., Guasch, H., Romani,
651 A.M., Sabater, S., 2010. Effects of a bactericide on the structure and survival of benthic
652 diatom communities. Vie et Milieu / Life & Environment 60, 109.

- 653 Neury-Ormanni, J., Vedrenne, J., Wagner, M., Jan, G., Morin, S., 2020. Micro-meiofauna
654 morphofunctional traits linked to trophic activity. *Hydrobiologia* 847, 2725–2736.
655 <https://doi.org/10.1007/s10750-019-04120-0>
- 656 Trauchan, M.A., Oriel, P.J., 2003. Degradation of benzyldimethylalkylammonium chloride by
657 *Aeromonas hydrophila* sp. K. *Journal of Applied Microbiology* 94, 266–272.
658 <https://doi.org/10.1046/j.1365-2672.2003.01829.x>
- 659 Pérez, P., Fernández, E., Beiras, R., 2009. Toxicity of Benzalkonium Chloride on Monoalgal
660 Cultures and Natural Assemblages of Marine Phytoplankton. *Water Air Soil Pollut* 201, 319–
661 330. <https://doi.org/10.1007/s11270-008-9947-x>
- 662 Perkin, E.K., Hölker, F., Richardson, J.S., Sadler, J.P., Wolter, C., Tockner, K., 2011. The influence of
663 artificial light on stream and riparian ecosystems: questions, challenges, and perspectives.
664 *Ecosphere* 2, art122. <https://doi.org/10.1890/ES11-00241.1>
- 665 Sozo-Antonio, J.S., Sanmartín, P., 2018. Exposure to artificial daylight or UV irradiation (A, B or C)
666 prior to chemical cleaning: an effective combination for removing phototrophs from granite.
667 *Biofouling* 34, 851–869. <https://doi.org/10.1080/08927014.2018.1512103>
- 668 Core Team (2020). — European Environment Agency [WWW Document], n.d. URL
669 [https://www.eea.europa.eu/data-and-maps/indicators/oxygen-consuming-substances-in-](https://www.eea.europa.eu/data-and-maps/indicators/oxygen-consuming-substances-in-rivers/r-development-core-team-2006)
670 [rivers/r-development-core-team-2006](https://www.eea.europa.eu/data-and-maps/indicators/oxygen-consuming-substances-in-rivers/r-development-core-team-2006) (accessed 10.31.22).
- 671 Rabenau, H.F., Kampf, G., Cinatl, J., Doerr, H.W., 2005. Efficacy of various disinfectants against
672 SARS coronavirus. *Journal of Hospital Infection* 61, 107–111.
673 <https://doi.org/10.1016/j.jhin.2004.12.023>
- 674 Takagami, Y., Yokoyama, H., Nishimura, H., Ose, Y., Tashima, T., 1989. Mechanism of resistance to
675 benzalkonium chloride by *Pseudomonas aeruginosa*. *Appl Environ Microbiol* 55, 2036–2040.
- 676 Severina, I.I., Muntyan, M.S., Lewis, K., Skulachev, V.P., 2001. Transfer of Cationic Antibacterial
677 Agents Berberine, Palmatine, and Benzalkonium Through Bimolecular Planar Phospholipid
678 Film and *Staphylococcus aureus* Membrane. *IUBMB Life* 52, 321–324.
679 <https://doi.org/10.1080/152165401317291183>
- 680 Singh, S.P., Singh, P., 2015. Effect of temperature and light on the growth of algae species: A
681 review. *Renew. Sustain. Energy Rev.* 50, 431–444.
682 <https://doi.org/10.1016/j.rser.2015.05.024>
- 683 Seevidya, V.S., Lenz, K.A., Svoboda, K.R., Ma, H., 2018. Benzalkonium chloride, benzethonium
684 chloride, and chloroxyleneol - Three replacement antimicrobials are more toxic than triclosan
685 and triclocarban in two model organisms. *Environmental Pollution* 235, 814–824.
686 <https://doi.org/10.1016/j.envpol.2017.12.108>
- 687 Sütterlin, H., Alexy, R., Kümmerer, K., 2008. The toxicity of the quaternary ammonium compound
688 benzalkonium chloride alone and in mixtures with other anionic compounds to bacteria in
689 test systems with *Vibrio fischeri* and *Pseudomonas putida*. *Ecotoxicology and Environmental*
690 *Safety* 71, 498–505. <https://doi.org/10.1016/j.ecoenv.2007.12.015>
- 691 Tamminen, M., Spaak, J., Tlili, A., Eggen, R., Stamm, C., Räsänen, K., 2022. Wastewater
692 constituents impact biofilm microbial community in receiving streams. *Science of The Total*
693 *Environment* 807, 151080. <https://doi.org/10.1016/j.scitotenv.2021.151080>
- 694 Tlili, A., Corcoll, N., Arrhenius, Å., Backhaus, T., Hollender, J., Creusot, N., Wagner, B., Behra, R.,
695 2020. Tolerance Patterns in Stream Biofilms Link Complex Chemical Pollution to Ecological
696 Impacts. *Environ. Sci. Technol.* 54, 10745–10753. <https://doi.org/10.1021/acs.est.0c02975>
- 697 Ugwu, C.U., Aoyagi, H., Uchiyama, H., 2007. Influence of irradiance, dissolved oxygen
698 concentration, and temperature on the growth of *Chlorella sorokiniana*. *Photosynthetica* 45,
699 309–311. <https://doi.org/10.1007/s11099-007-0052-y>

700 United States Environmental Protection Agency 2006. Reregistration eligibility decision for alkyl
701 dimethyl benzyl ammonium chloride. (<https://nepis.epa.gov>). Accessed on 17 Feb. 2021.

702 EPA, O., 2020. About List N: Disinfectants for Coronavirus (COVID-19) [WWW Document]. URL
703 <https://www.epa.gov/coronavirus/about-list-n-disinfectants-coronavirus-covid-19-0>
704 (accessed 10.31.22).

705 van Wijk, D., Gyimesi-van den Bos, M., Gattener-Arends, I., Geurts, M., Kamstra, J., Thomas, P.,
706 2009. Bioavailability and detoxification of cationics: I. Algal toxicity of alkyltrimethyl
707 ammonium salts in the presence of suspended sediment and humic acid. *Chemosphere* 75,
708 303–309. <https://doi.org/10.1016/j.chemosphere.2008.12.047>

709 Vassenaar, T., Ussery, D., Nielsen, L., Ingmer, H., 2015. Review and phylogenetic analysis of qac
710 genes that reduce susceptibility to quaternary ammonium compounds in *Staphylococcus*
711 species. *European Journal of Microbiology and Immunology* 5, 44–61.
712 <https://doi.org/10.1556/eujmi-d-14-00038>

713 Yang, Z., Geng, L., Wang, W., Zhang, J., 2012. Combined effects of temperature, light intensity,
714 and nitrogen concentration on the growth and polysaccharide content of *Microcystis*
715 *aeruginosa* in batch culture. *Biochem. Syst. Ecol.* 41, 130–135.
716 <https://doi.org/10.1016/j.bse.2011.12.015>

717 Yin, H., Wang, Lingling, Zeng, G., Wang, Longfei, Li, Y., 2022. The Roles of Different Fractions in
718 Freshwater Biofilms in the Photodegradation of Methyl Orange and Bisphenol A in Aqueous
719 Solutions. *Int. J. Environ. Res. Public Health* 19, 12995.
720 <https://doi.org/10.3390/ijerph192012995>

721 Zhang, C., Cui, F., Zeng, G., Jiang, M., Yang, Z., Yu, Z., Zhu, M., Shen, L., 2015. Quaternary
722 ammonium compounds (QACs): A review on occurrence, fate and toxicity in the
723 environment. *Science of The Total Environment* 518–519, 352–362.
724 <https://doi.org/10.1016/j.scitotenv.2015.03.007>

725 Zulu, N.N., Zienkiewicz, K., Vollheyde, K., Feussner, I., 2018. Current trends to comprehend lipid
726 metabolism in diatoms. *Progress in Lipid Research* 70, 1–16.
727 <https://doi.org/10.1016/j.plipres.2018.03.001>

728
729
730
731
732
733
734
735
736
737
738
739
740
741
742
743
744
745

746
747
748
749
750
751
752
753

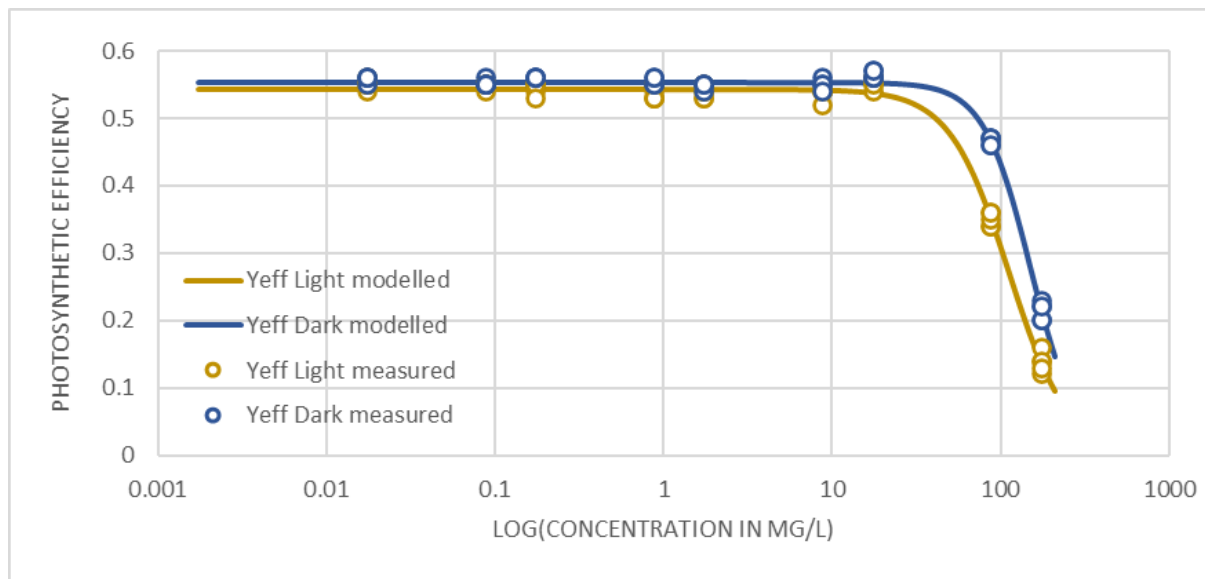
754 **Appendices**

755 **A- Preliminary experiment**

756

757 This preliminary experiment aimed to test the sensitivity of our biofilm to
758 dodecylbenzyltrimethylammonium (BAC 12) to select a sub-lethal concentration to be used
759 in the main experiment. We ran a dose-response experiment in which we tested nine
760 concentrations ranging between $17.5 \mu\text{g.L}^{-1}$ and 175mg.L^{-1} (following a logarithmic increase)
761 for 4 hours. Each concentration was tested twice, one test at a mean light level of 16.86
762 $\mu\text{mol.s.m}^{-2}$ and the other kept in the dark.

763 Glass slides ($26.5 \text{ cm} \times 6 \text{ cm}$) colonized by biofilms for three months were scraped and the
764 biofilms put into 500 mL of water. For each concentration, we contaminated 1.5 mL of the
765 biofilm solution. After four hours of contamination, we analysed the photosynthetic
766 efficiency of the samples with a Phyto-PAM (see section 2.3).



767

768 **Figure A. Dose-Response curve for photosynthetic efficiency in biofilms exposed to light or dark and**
769 **increasing BAC concentration for 4 hours. YeFF = Photosynthetic efficiency.**

770

771 The dose-response curve give us an EC_{50} of $112 \pm 3 \text{ mg.L}^{-1}$ and a EC_5 of $34 \pm 3 \text{ mg.L}^{-1}$ for
772 photosynthesis inhibition in biofilm exposed to light. For the biofilm kept in obscurity, we
773 found EC_{50} of $151 \pm 3 \text{ mg.L}^{-1}$ and a EC_5 of $58 \pm 3 \text{ mg.L}^{-1}$. This result allowed us to choose the

774 concentration of 30 mg.L⁻¹ for the 10 days biofilm exposure which is the lowest
775 concentration with a minimum effect on photosynthetic efficiency.

776

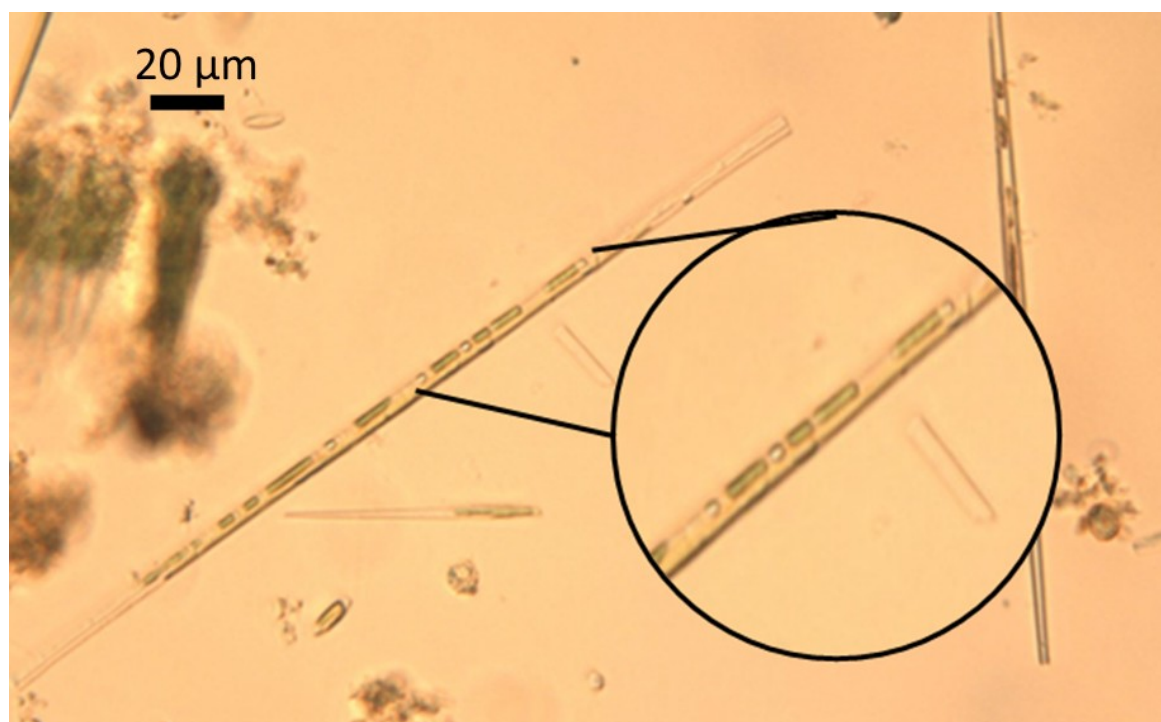
777

778

779

780 **B- Effects of BAC 12 on chloroplasts**

781



782

783 **Figure B.1. Chloroplasts of diatoms in non-contaminated biofilm. x400 magnification**

784



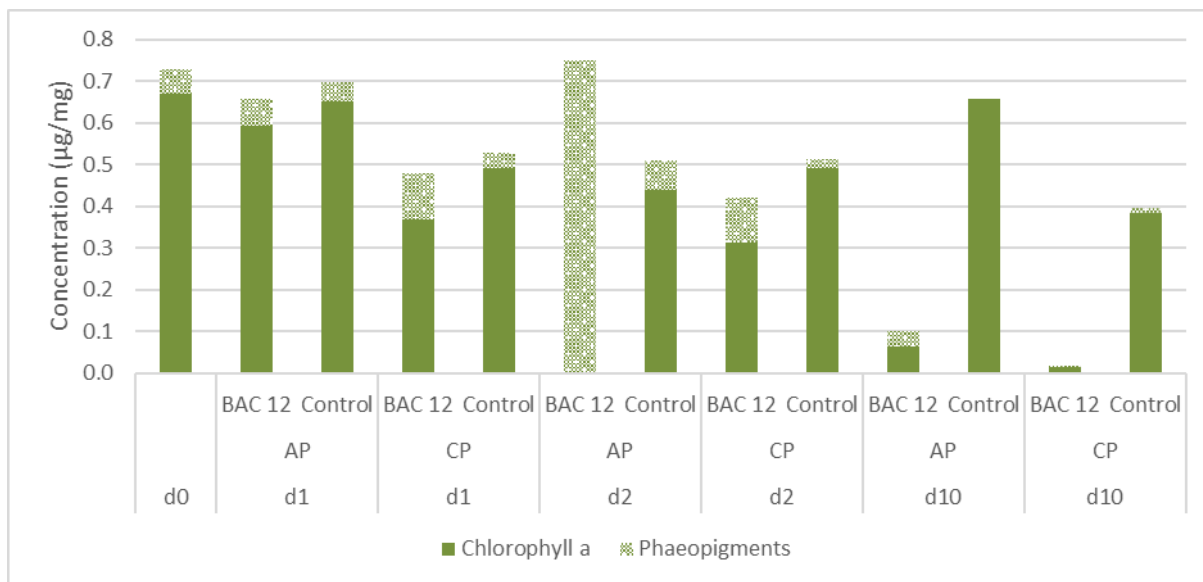
785

786 **Figure B.2. Chloroplasts of diatoms in BAC 12 contaminated biofilm after 10 days of exposure. x400**
 787 **magnification.**

788

789 **C- Pigment analysis**

790



791

792 **Figure C. Pigment analysis. n = 1. BAC 12 = contaminated biofilm; Control = non-exposed biofilm; AP =**
 793 **alternated photoperiod; CP = continuous photoperiod.**

794

795 Although the pigment analyses were only performed on one replicate, we can see that
 796 chlorophyll *a* concentrations are lower in the BAC 12 contaminated samples than in the

797 control samples. At d2, we see that there is no chlorophyll a in the contaminated samples for
798 AP but only phaeopigments. At the end of the experiment, there were very low pigment
799 concentrations in contaminated samples. Due to the lack of replicates, we cannot assess
800 whether there were significant effects of light conditions, BAC 12 contamination or any
801 interaction between light, BAC 12 and/or time on chlorophyll *a* or phaeopigment levels.

802

803

804

805

806

807

808

809

810

811

812 **D- HPLC gradients for the lipidomic analysis**

813

814 **Table D.1. HPLC gradients for phospholipid and glycolipid analysis.**

815

Time (min)	40 mmol.L ⁻¹ Ammonium acetate buffer (%)	Acetonitrile (%)
0	5	95
2	5	95
7	30	70
10	30	70
11	5	95

13.7	5	95
------	---	----

816

817

Table D.2. HPLC gradients for triglyceride analysis.

818

Time (min)	Solvent A* (%)	Solvent B* (%)
0	50	50
0.3	50	50
5.3	1	99
7.3	1	99
8.3	50	50
9.8	50	50

819 * Solvent A: solution of acetonitrile/water/40 mmol.L⁻¹ ammonium acetate buffer
820 (600/390/10, v/v/v)

821 Solvent B: solution of isopropanol/acetonitrile/1 mol.L⁻¹ ammonium acetate buffer
822 (900/90/10, v/v/v)

823

824 **E- Lipid standards**

825 Polar lipid standards were purchased from Avanti Polar Lipids. Quantitations of
826 phosphatidylcholine (PC), phosphatidylethanolamine (PE) and phosphatidylglycerol (PG)
827 were respectively carried out with 1-palmitoyl-2-oleoyl-glycero-3-phosphocholine or PC
828 (16:0/18:1) (850457), 1-palmitoyl-2-oleoyl-sn-glycero-3-phosphoethanolamine or PE
829 (16:0/18:1) (850757), and 1-palmitoyl-2-oleoyl-sn-glycero-3-phospho-(1'-rac-glycerol) or PG
830 (16:0/18:1) (840457).

831 For glycolipids, monogalactosyldiacylglycerol (840523), digalactosyldiacylglycerol (840524)
832 and sulfoquinovosyldiacylglycerol (840525) from plant extracts were used as standards.
833 Quantitation was performed with the following molecular species: MGDG (16:3_18:3) (63%

834 of the total MGDG standard), DGDG (18:3_18:3) (22% of the total MGDG standard), and
835 SQDG (34:3) (78% of the total MGDG standard).

836 1,2-diheptadecanoyl-sn-glycero-3-phosphocholine or PC (2x17:0) (850360) was used as
837 internal standard for PC phospholipids, 1,2-diheptadecanoyl-sn-glycero-3-
838 phosphoethanolamine or PE (2x17:0) (830756) was used as internal standard for PE
839 phospholipids, and 1,2-diheptadecanoyl-sn-glycero-3-phospho-(1'-rac-glycerol) or PG
840 (2x17:0) (830456) was used as internal standard for PG phospholipids, and both MGDG,
841 DGDG and SQDG glycolipids.

842 1,2-dipalmitoyl-sn-glycero-3-O-4'-(N,N,N-trimethyl)-homoserine or DGTS (2x16:0) (857464)
843 was used for the diacylglyceryltrimethylhomo-Ser (DGTS) lipids. 1,2-dipalmitoyl-sn-glycero-3-
844 O-4'-[N,N,N-trimethyl(d9)]-homoserine or DGTS-d9 (2x16:0) (857463) was used as internal
845 standard for DGTS lipids

846 Triglycerides were purchased from Sigma-Aldrich. Tristearin or TAG (3x18:0) (≥99%, T5016)
847 was used as the calibration standard while TAG (3x17:0) (≥99%, T2151) was used as the
848 internal standard.

849

850

851

852 **F- Mass spectrometry parameters for lipid analysis**

853

854 **Table F.1. Mass spectrometry parameters for phospholipid and glycolipid analysis.**

855

	Curtain gas	CAD	IonSpray	Temperature	Ion source gas 1	Ion source gas 2	Declustering potential	Collision energy
MGDG	30 psi	3	-4500 V	450°C	30 psi	60 psi	-61 V	-28 V
DGDG	30 psi	3	-4500 V	450°C	30 psi	60 psi	-61 V	-28 V
SQDG	30 psi	3	-4500 V	450°C	30 psi	60 psi	-126 V	-66 V
PE	30 psi	3	-4500 V	450°C	30 psi	60 psi	-50 V	-50 V

PG	30 psi	3	-4500 V	450°C	30 psi	60 psi	-100 V	-50 V
PC	30 psi	3	-4500 V	450°C	30 psi	60 psi	-100 V	-50 V

856

857

858

Table F.2. Mass spectrometry parameters for triglyceride analysis.

	Curtain gas	CAD	IonSpray	Temperature	Ion source gas 1	Ion source gas 2	Declustering potential	Collision energy
Triglycerides	30 psi	3	+5000 V	450°C	30 psi	45 psi	50 V	38 V

859